

Thermoelectric Misfit-Layered Cobalt Oxides (II): Properties of Oxygen-Controlled Samples of $\text{Ca}_3\text{Co}_{3.95}\text{O}_{9+\delta}$

Teruki Motohashi, Takuya Konno, Toyomi Aoyama,
Maarit Karppinen, and Hisao Yamauchi

Materials and Structures Laboratory, Tokyo Institute of Technology, Yokohama 226-8503, Japan

Fax: 81-45-924-5318, e-mail: t-mot@msl.titech.ac.jp

Properties of the misfit-layered cobalt oxide, $[\text{Ca}_2\text{CoO}_{3-\varepsilon}]_q\text{CoO}_2$ (*i.e.* $\text{Ca}_3\text{Co}_{3.95}\text{O}_{9+\delta}$), were systematically studied with respect to oxygen nonstoichiometry. Samples with $\delta = -0.05 \sim 0.29$ were prepared by post-annealing an air-synthesized material in flowing N_2 and also in high-pressure oxygen atmosphere. With increasing oxygen content, δ , the *b*-axis length of the rock-salt layer systematically increased while the *b*-axis length of the CoO_2 layer remained unchanged. It was found that (1) the semiconductive behavior of the samples with $\delta \leq 0.00$ is suppressed by oxygen doping, and (2) a magnetic transition appears at $T_m \approx 20$ K only for the samples with $\delta \geq 0.24$. Thus it has been revealed that the properties of $\text{Ca}_3\text{Co}_{3.95}\text{O}_{9+\delta}$ are strongly dependent on oxygen nonstoichiometry.

Key words: misfit-layered cobalt oxide, $\text{Ca}_3\text{Co}_{3.95}\text{O}_{9+\delta}$, oxygen nonstoichiometry, thermoelectric properties

1. INTRODUCTION

Misfit-layered cobalt oxides, $[\text{M}_m\text{A}_2\text{O}_{m+2-\varepsilon}]_q\text{CoO}_2$, have attracted much attention. The compounds exhibit large thermoelectric power and low resistivity simultaneously ($S > 100 \mu\text{V}/\text{K}$ and $\rho < 10^{-2} \Omega \text{ cm}$ at 300 K) [1-8], which has made them promising candidates for thermoelectric applications. The crystal structure of the misfit-layered cobalt oxides consists of a triangular CoO_2 layer coupled incoherently with a rock-salt-type (RS) $\text{AO}-(\text{MO})_m\text{-AO}$ block (*M*: transition metal and/or heavy metal, *A*: alkali-earth element). It is believed that the triangular CoO_2 layer as a common building block plays the key role in realizing the superb thermoelectric characteristics.

Recently, Koshibae *et al.* [9] theoretically treated thermoelectric power of cobalt oxides by generalizing the Heikes formula, and suggested that the observed large magnitude of thermoelectric power would be originated from both the large degeneracy of cobalt species and the strong correlation of *3d* electrons. They concluded that the high-temperature limit of thermoelectric power of such a compound is given by

$$S = -\frac{k_B}{e} \ln\left(\frac{g_3}{g_4} \frac{c}{1-c}\right) \quad (1)$$

where *c*, *g*₃, and *g*₄ denote the concentration of Co^{IV} ions and the degrees of degeneracy for Co^{III} and Co^{IV} , respectively. From this formula, it is found that the thermoelectric power strongly depends on the average valence of cobalt. Therefore, it is of particular interest to see how the cobalt valence affects the thermoelectric properties of the misfit-layered cobalt oxides.

The oxygen-content control for oxide materials is one of the conventional ways to tune the valence state of the constituent metal ions. Recently, we precisely determined the oxygen content and accordingly the

cobalt valence for four kinds of misfit-layered or related cobalt oxides, *i.e.* $\text{Ca}_3\text{Co}_{3.95}\text{O}_{9+\delta}$, $(\text{Bi,Pb})_{2.1}\text{Sr}_{2.15}\text{Co}_2\text{O}_{8+\delta}$, $\text{Pb}_{0.35}\text{SrCo}_{1.05}\text{O}_{3+\delta}$, and $\text{Na}_x\text{CoO}_{2+\delta}$ [10]. It was found that only for $\text{Ca}_3\text{Co}_{3.95}\text{O}_{9+\delta}$ oxygen-content tunability is possible. This compound possesses a composite crystal structure that consists of the CoO_2 layer and a triple rock-salt-type CaO-CoO-CaO block [5,11], *i.e.* *A* and *M* in the general formula correspond to Ca and Co, respectively. In the present study, we have investigated the thermoelectric and magnetic properties of a series of oxygen-content controlled samples of $\text{Ca}_3\text{Co}_{3.95}\text{O}_{9+\delta}$ to elucidate the influence of oxygen nonstoichiometry on the properties of this compound.

2. EXPERIMENTAL

The samples were prepared by a conventional solid-state reaction method. A powder mixture of CaCO_3 and Co_3O_4 with an appropriate ratio was fired twice at 900°C (for 20 hours each) in air, first in powder form and then as a pellet. The actual composition of the single-phase sample was examined by inductively coupled plasma atomic emission spectroscopy (ICP-AES; Seiko Instruments, SPS-1500VR) and determined at Ca : Co = 3.00 : 3.95±0.05. This cation ratio is in good agreement with the estimated value based on the reported composite crystal structure, *i.e.* $[\text{Ca}_2\text{CoO}_3]_{0.62}\text{CoO}_2 \approx \text{Ca}_3\text{Co}_{3.92}\text{O}_{9.34}$ [11].

The oxygen content δ was controlled by the temperature-controlled oxygen-depletion (TCOD) method [12]. In the TCOD method, as-air-synthesized samples of 100 mg were annealed in flowing N_2 gas at various pre-decided temperatures in a thermobalance (MAC Science, TG/DTA 2000S), followed by a rapid cooling to room temperature. A high-pressure oxygen annealing was also performed in 90 atm O_2 at 400°C for 24 hours to obtain the maximum oxygen-content sample. All the samples prepared were checked for phase purity by x-ray powder diffraction using a MAC Science

M18XHF22 diffractometer with Cu-K_α radiation. The absolute oxygen contents were determined by cerimetric and/or iodometric titrations. A more detailed description of the experimental procedure is given elsewhere [10].

Electron diffraction (ED) patterns were taken using a TEM (Hitachi, H-9000NAR) with an acceleration voltage of 300 kV. Resistivity measurements were performed using a four-point-probe apparatus (Quantum Design, PPMS). Thermoelectric power was measured using a steady-state technique with a typical temperature gradient of 0.5 K/cm. Magnetization was measured by a SQUID magnetometer (Quantum Design, MPMS-XL).

3. RESULTS AND DISCUSSION

3.1 Oxygen nonstoichiometry

Figure 1 shows thermogravimetric (TG) curves of a series of $\text{Ca}_3\text{Co}_{3.95}\text{O}_{9+\delta}$ samples obtained with different oxygen contents through TCO annealings. The oxygen depletion was found to occur gradually up to $\sim 750^\circ\text{C}$ (with an onset about 400°C). All the samples were annealed at the final temperature for a long period enough to attain the thermodynamic equilibrium. The observed weight-losses corresponded to oxygen losses of $\Delta\delta = 0.04(5)$, $0.15(5)$, $0.17(5)$, and $0.25(5)$, respectively. When heated above 750°C in N_2 , this compound was found to decompose to a mixture of $\text{Ca}_3\text{Co}_2\text{O}_6$ and CoO . Therefore, the 750°C -annealed sample should have an oxygen content close to the lowest limit.

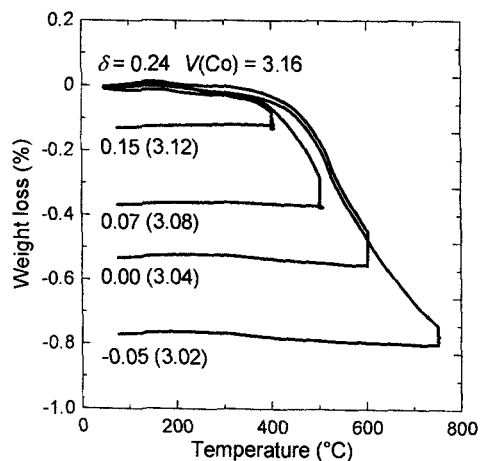


Fig. 1. TCO annealings performed in a thermobalance in N_2 gas to obtain oxygen-controlled samples of $\text{Ca}_3\text{Co}_{3.95}\text{O}_{9+\delta}$.

Oxygen contents determined by cerimetric and iodometric titration methods are summarized in Table I. The calculated average cobalt valence, $V(\text{Co})$, is also presented. It is not observed that one titration technique would systematically give smaller or larger values than the other. This is an indication of high accuracy of the wet-chemical redox analyses in the present study. The oxygen-content variation, $\Delta\delta$, is as large as 0.34, being much larger than those for other misfit-layered cobalt oxides [10]. Since there are two different cobalt sites in $\text{Ca}_3\text{Co}_{3.95}\text{O}_{9+\delta}$, i.e. $\text{Co}(\text{CoO}_2)$ and $\text{Co}(\text{RS})$, $V(\text{Co})$ in Table I is the average value of the two sites.

Table I. Results of the oxygen content analyses carried out by cerimetric (c) and iodometric (i) titration, for overall oxygen content (δ) and the average valence of cobalt ($V(\text{Co})$) in the $\text{Ca}_3\text{Co}_{3.95}\text{O}_{9+\delta}$ samples.

| Annealing condition | Oxygen content δ | Co valence $V(\text{Co})$ |
|----------------------------------|-------------------------|---------------------------|
| 90 atm O_2 | 0.29 (i) | 3.19 |
| As-air-synthesized | 0.23 (c) / 0.25 (i) | 3.15 / 3.17 |
| N_2 400°C | 0.15 (c) | 3.12 |
| N_2 500°C | 0.05 (c) / 0.08 (i) | 3.07 / 3.08 |
| N_2 600°C | 0.00 (c) / 0.00 (i) | 3.04 / 3.04 |
| N_2 750°C | -0.03 (c) / -0.06 (i) | 3.02 / 3.01 |

The lattice parameters a , b for the RS layer (b_{RS}), c , and β were determined by x-ray powder diffraction. The b -axis length for the CoO_2 layer (b_{CoO_2}) was obtained from the misfit ratio ($q \equiv b_{\text{CoO}_2} / b_{\text{RS}}$) determined by the ED analysis. The lattice parameters are plotted in Fig. 2 as a function of oxygen content. The a -axis length remained nearly constant for all the samples. On the other hand, the b_{RS} - and c -axis length, respectively, increases and decreases with increasing δ . Thus, the lattice expansion is anisotropic with respect to the oxygen-content variation. It is also noted that the value of b_{CoO_2} is less dependent on the oxygen content as compared to b_{RS} .

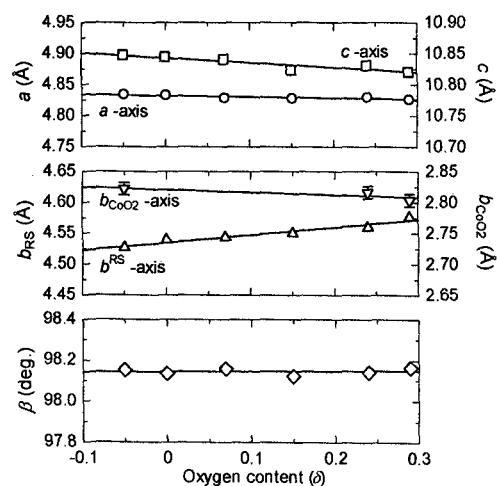


Fig. 2. Lattice parameters a , b for the RS layer (b_{RS}), b for the CoO_2 layer (b_{CoO_2}), c , and β for the $\text{Ca}_3\text{Co}_{3.95}\text{O}_{9+\delta}$ samples with respect to the oxygen content (δ).

3.2 Electrical resistivity and thermoelectric power

Figure 3(a) shows the dependence of electrical resistivity (ρ) on temperature for the $\text{Ca}_3\text{Co}_{3.95}\text{O}_{9+\delta}$ samples with various oxygen contents. The room-temperature ρ values are smaller than $1 \Omega \text{ cm}$ for all the samples. The ρ value tends to be enhanced with decreasing oxygen content. Some samples do not follow this trend, but this is probably due to the grain-boundary effect. In Fig. 3(b), shown are the $\rho - T$ curves that have been normalized by the ρ values at 350 K. Two highly reduced samples, $\delta = -0.05$ and 0.00 , are semiconductive in a temperature range of 4 – 350 K, while a metallic-to-semiconductive crossover appears for the samples with $\delta \geq 0.07$. The crossover temperature where resistivity possesses the minimum

value (indicated by arrows in Fig. 3(b)) systematically increases with decreasing δ .

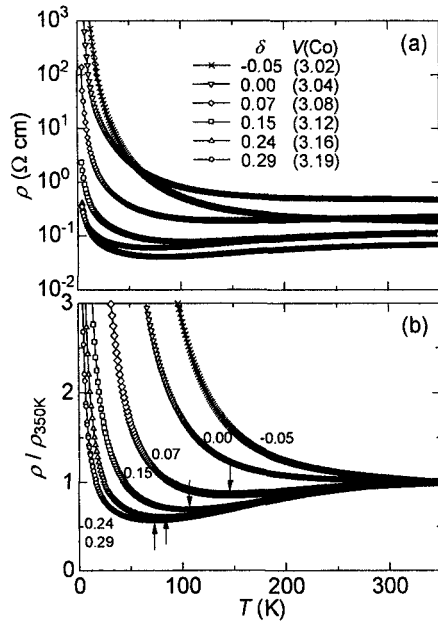


Fig. 3. (a) Temperature dependence of (a) ρ and (b) normalized ρ for the $\text{Ca}_3\text{Co}_{3.95}\text{O}_{9+\delta}$ samples. The ρ - T curves were normalized by the values at 350 K. The metallic-to-semiconductive crossover temperature where resistivity possesses the minimum value is indicated by an arrow.

Thermoelectric power (S) values for the $\delta = 0.29, 0.24, 0.07$, and -0.05 samples are plotted in Fig. 4. The absolute value of the room-temperature S for the as-air-synthesized sample (i.e. $\delta = 0.24$) is in good agreement with those reported in previous works [3,5]. The S value systematically increases with decreasing oxygen content (δ): $S = 133, 139, 163$, and $195 \mu\text{V} / \text{K}$ at 300 K for $\delta = 0.29, 0.24, 0.07$, and -0.05 , respectively. Using the ρ and S values, the thermoelectric power factor, defined as $P \equiv S^2 / \rho$, was calculated at 0.19, 0.30, 0.14, and $0.20 \mu\text{W} / \text{K cm}$ at 300 K for $\delta = 0.29, 0.24, 0.07$, and -0.05 , respectively. No significant improvement of the P value was obtained by the oxygen-content control. This is because the contribution of the enhanced thermoelectric power was cancelled out by the increase in resistivity.

It is of interest to see whether the enhanced thermoelectric power can be theoretically explained using Eq. (1). In the inset of Fig. 4, the observed S at 300 K (S_{obs}) and high-temperature limit of S by Eq. (1) (S_{HT}) are plotted as a function of $V(\text{Co})$. To calculate the S_{HT} value, we considered the low-spin states for both Co^{III} and Co^{IV} , i.e. g_3 and g_4 in Eq. (1) are 1 and 6, respectively [9]. It can be seen that S_{HT} (a solid curve) is much larger than S_{obs} (solid circles). Assuming that thermoelectric power at 300 K does not reach the high-temperature limit and the magnitude of S_{HT} is proportional to the $S_{300\text{K}}$ value, we multiplied the S_{obs} value by a factor of $S_{\text{HT}} / S_{\text{obs}}$ for the $\delta = 0.29$ sample to obtain "estimated S_{HT} ". The estimated S_{HT} , shown with open circles in the figure, is smaller than S_{HT} by Eq. (1),

in particular when $V(\text{Co})$ is close to 3.0. One possible reason for this discrepancy would be due to the inhomogeneous distribution of hole carriers between the RS and CoO_2 layers. Since the transport properties are considered to be mainly governed by the CoO_2 layer, the S_{pred} value should be calculated using a CoO_2 -layer-specific $V(\text{Co})$ value.

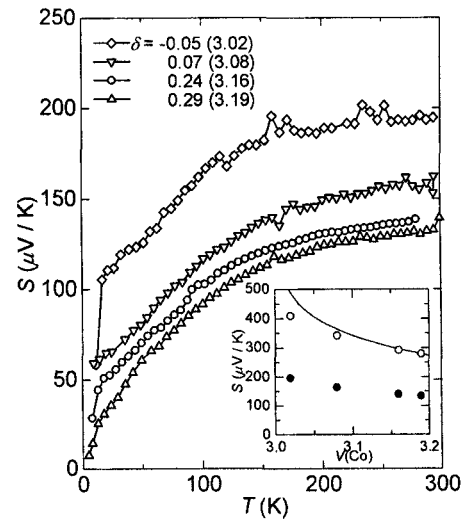


Fig. 4. Dependence of thermoelectric power (S) on temperature for the $\text{Ca}_3\text{Co}_{3.95}\text{O}_{9+\delta}$ samples with $\delta = 0.29, 0.24, 0.07$, and -0.05 . In the inset, observed S at 300 K (S_{obs}) and high-temperature limit of S by Eq. (1) (S_{HT}) are plotted as a function of the cobalt valence [$V(\text{Co})$]. Solid circles and a solid curve denote S_{obs} and S_{HT} , respectively. Open circles represent the "estimated S_{HT} " calculated from the experimental data (see text).

3.3 Magnetic properties

Figure 5 shows the dependence of magnetic susceptibility (χ) on temperature for the samples with various oxygen contents. For $\delta = 0.29$ and 0.24 , magnetic susceptibility rapidly increases below $T_m \approx 22$ K, indicating that a magnetic transition occurs at this temperature. At 5 K, a large hysteresis loop that is related to the magnetic transition was seen for these oxygenated samples. The magnetic transition was also seen for as- O_2 -synthesized samples in previous reports [3,13]. The magnetic transition disappeared when the oxygen content was decreased. Samples with $\delta \leq 0.15$ are paramagnetic down to 5 K.

It is thus found that only oxygenated samples show a magnetic transition at $T_m \approx 20$ K. As a possible explanation for the disappearance of magnetic ordering, the effect of oxygen vacancies in the RS layer is suggested. In fact, many oxygen vacancies are considered to exist in reduced samples; for instance, taking into consideration the composite chemical formula for the $\delta = -0.05$ sample, $[\text{Ca}_2\text{CoO}_{3-\varepsilon}]_{0.62}\text{CoO}_2$, the ε value should be ≈ 0.3 . Since the magnetic ordering is believed to occur within the RS layer [14], it is likely that such a large amount of oxygen vacancies in the RS layer disrupt the superexchange interaction between cobalt spins, resulting in the disappearance of magnetic ordering.

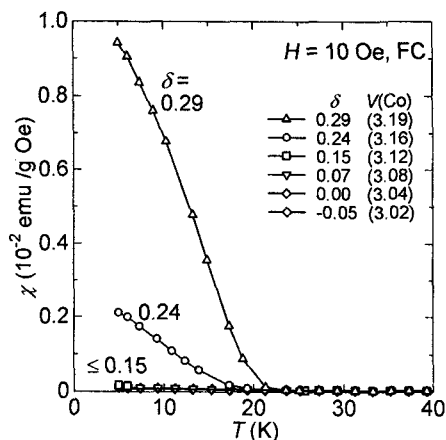


Fig. 5. Dependence of magnetic susceptibility (χ) on temperature for the $\text{Ca}_3\text{Co}_{3.95}\text{O}_{9+\delta}$ samples.

4. CONCLUSION

Properties of the misfit-layered cobalt oxide, $[\text{Ca}_2\text{CoO}_{3-\epsilon}]_q\text{CoO}_2$ (*i.e.* $\text{Ca}_3\text{Co}_{3.95}\text{O}_{9+\delta}$), were systematically studied with respect to oxygen nonstoichiometry. The oxygen content was controlled by the temperature-controlled oxygen-depletion (TCOD) method and also by high-pressure oxygen annealing. The δ value was precisely determined by wet-chemical redox titration techniques. Samples with various oxygen contents in the range of $\delta = -0.05 \sim 0.29$ were successfully prepared. The oxygen-content variation, $\Delta\delta$, was determined at 0.34, being much larger than those for other misfit-layered cobalt oxides. With increasing oxygen content, the *b*-axis length of the rock-salt layer systematically increased while the *b*-axis length of the CoO_2 layer remained unchanged. It was found that (1) the semiconductive behavior of the samples with $\delta \leq 0.00$ is suppressed by oxygen doping, and (2) a magnetic transition appears at $T_m \approx 20$ K only for the samples with $\delta \geq 0.24$. Thus it has been revealed that the properties of $\text{Ca}_3\text{Co}_{3.95}\text{O}_{9+\delta}$ are strongly dependent on oxygen nonstoichiometry.

REFERENCES

- [1] T. Ito, T. Kawata, T. Kitajima, and I. Terasaki, in *Proceedings of the 17th International Conference on Thermoelectrics (ICT '98)*, Nagoya, Japan (1998) pp. 595-597.
- [2] R. Funahashi, I. Matsubara, and S. Sodeoka, *Appl. Phys. Lett.* **76**, 2385 (2000).
- [3] Y. Miyazaki, K. Kudo, M. Akoshima, Y. Ono, Y. Koike, and T. Kajitani, *Jpn. J. Appl. Phys.* **39**, L531 (2000).
- [4] R. Funahashi, I. Matsubara, H. Ikuta, T. Takeuchi, U. Mizutani, and S. Sodeoka, *Jpn. J. Appl. Phys.* **39**, L1127 (2000).
- [5] A.C. Masset, C. Michel, A. Maignan, M. Hervieu, O. Toulemonde, F. Studer, and B. Raveau, *Phys. Rev. B* **62**, 166 (2000).
- [6] S. Hébert, S. Lambert, D. Pelloquin, and A. Maignan,

Phys. Rev. B **64**, 172101 (2001).

[7] A. Maignan, L.B. Wang, S. Hébert, D. Pelloquin, and B. Raveau, *Chem. Mater.* **14**, 1231 (2002).

[8] D. Pelloquin, A. Maignan, S. Hébert, C. Michel, and B. Raveau, *J. Solid State Chem.* **170**, 374 (2003).

[9] W. Koshibae, K. Tsutsui, and S. Maekawa, *Phys. Rev. B* **62**, 6869 (2000).

[10] Y. Morita, J. Poulsen, T. Motohashi, T. Fujii, I. Terasaki, H. Yamauchi, and M. Karppinen, *Chem. Mater.* submitted.

[11] Y. Miyazaki, M. Onoda, T. Oku, M. Kikuchi, Y. Ishii, Y. Ono, Y. Morii, and T. Kajitani, *J. Phys. Soc. Jpn.* **71**, 491 (2002).

[12] M. Karppinen and H. Yamauchi, in *International Book Series: Studies of High Temperature Superconductors*, **37**, A.V. Narlikar (Ed.) (Nova Science Publishers, New York 2001) pp. 109-143.

[13] J. Sugiyama, H. Itahara, T. Tani, J.H. Brewer, E.J. Ansaldo, *Phys. Rev. B* **66**, 134413 (2002).

[14] Y. Miyazaki, private communication.

(Received October 13, 2003; Accepted January 16, 2004)